

Mid-Infrared Diffuse Reflection on Ultrafast Time Scales

Eric B. Brauns

Department of Chemistry, University of Idaho, Moscow, ID 83843 USA

This paper describes an instrument capable of studying diffuse reflection of mid-infrared (mid-IR) photons on ultrafast time scales. Femtosecond mid-IR pulses are generated by difference frequency mixing the output of an optical parametric amplifier that is pumped using a regeneratively amplified Ti:Sapphire laser. Time resolution is achieved by up-converting the diffusely reflected photons with pulses from the Ti:Sapphire oscillator. Experiments were performed on a series of powdered KBr samples containing varying amounts of carbon black. The results suggest that diffusely reflected mid-IR photons fall into two distinct categories. A small fraction of the photons travel relatively long effective path lengths (1.3–2.3 mm), while the majority traverse a much shorter distance (0.2–0.05 mm).

Index Headings: **Ultrafast; Diffuse reflection; Mid-infrared; Mid-IR; Up-conversion.**

INTRODUCTION

Diffuse reflection (DR) occurs when light penetrates a translucent scattering solid (e.g., a powder comprised of a finely ground crystalline material) and is reemitted after undergoing multiple instances of reflection and refraction.^{1,2} A schematic of this process is shown in Fig. 1. As a result of repeated cycles of transmission/reflection, photons can travel long distances through powdered samples. As they do so, they interact with multiple particles as well as the same particles multiple times. As a consequence of these multiple interactions, the net absorption of a weakly absorbing analyte, or one that is present at low concentration in a transparent matrix, can be increased many-fold. Indeed, DR spectrometry is a well-known sampling technique in mid-infrared (mid-IR) and near-IR spectroscopy.^{1,2} Despite its significance, little is known about the underlying mechanism—particularly mid-infrared DR.

An important parameter in DR is the effective path length that the photons travel; the longer the path length, the greater the sensitivity to trace analytes. The first study to determine the effective path length of diffusely reflected IR photons was done by Averett and Griffiths.³ They studied the concentration-dependent DR spectrum

of low concentrations of caffeine dispersed in KBr. Using an extension of Beer's law, they indirectly determined that the average path length in pure KBr was ~ 4 mm and that it decreased as the concentration of the caffeine was increased. Since the photons have to travel into and then out of the sample, this seemed to suggest that the average penetration depth was ~ 2 mm. However, they showed that the ~ 4 mm overall path was actually highly random and that the actual penetration depth was less than 0.5 mm.

A direct determination of the effective path length requires a time-resolved approach.^{4–9} By measuring the time for photons to traverse the sample, it is straightforward to determine the distance they traveled. However, time-resolved techniques are complicated and can pose unique challenges. This is especially true for mid-IR spectroscopy, where the detectors tend to be quite slow and not as sensitive as their visible and near-IR counterparts. This paper describes an experimental setup designed to mitigate these issues. Time resolution is achieved by “up-converting” the diffusely reflected light with a short laser pulse that acts as a gate. Up-conversion is an optical timing technique that circumvents the otherwise slow electronic circuitry of mid-IR detectors.¹⁰ Moreover, the up-converted signal lies in the visible region of the spectrum where sensitive photomultiplier tubes or charge-coupled devices can be used.

EXPERIMENTAL

Instrument Overview. A schematic of the instrument is shown in Fig. 2. The system is based on a 1 kHz regeneratively amplified Ti:Sapphire laser (Libra HE, Coherent). The amplified Ti:Sapphire produces ~ 3 mJ pulses at a central wavelength of ~ 791 nm with a nominal pulse width of 100 fs. These pulses were separated into two beam paths using a 95% reflective beam splitter. The transmitted beam (5%, ~ 150 μ J) was passed through a computer controlled optical delay (ANT-95, Aerotech) and used as the gate to up-convert the diffusely reflected mid-IR photons. The reflected beam (95%, ~ 2.9 mJ) was used to pump an optical parametric amplifier (Coherent, OPerA) fitted with a difference frequency generation add-on module. The combined optical parametric amplifier/difference frequency generator produced ~ 30 μ J pulses (~ 120 fs)

Received 19 August 2013; accepted 11 October 2013.

E-mail: ebrauns@uidaho.edu.

DOI: 10.1366/13-07258

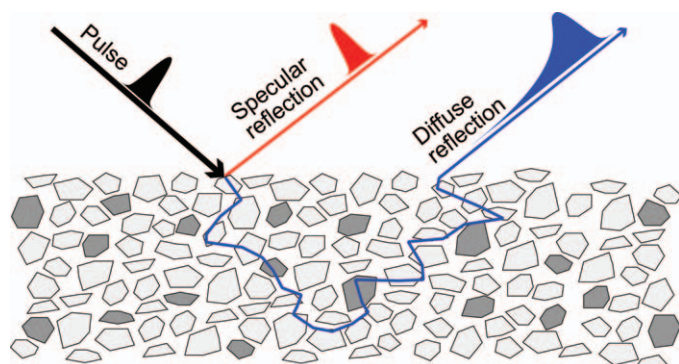


FIG. 1. An illustration of diffuse reflection. A short laser pulse (shown in black) is incident on a sample comprised of a translucent powder (light gray shapes), which could have trace amounts of an absorbing species present (dark gray shapes). Specular reflection (shown in red) occurs when the light simply reflects off of the initial surface. In this case, the pulse is left relatively unchanged. However, some of the light enters the sample and undergoes multiple instances of reflection and refraction before being reemitted from the sample. This is diffuse reflection (shown in blue). The pulse is broadened in time because of the longer path length.

centered at a wavelength of $5.8 \mu\text{m}$ (1720 cm^{-1}). A gold-coated 30° off-axis parabolic mirror ($f = 50.8 \text{ mm}$) was used to direct the mid-IR pulses toward the sample. The diffusely reflected light was collected and collimated using a second (identical) parabolic mirror. A third parabolic mirror (90° off-axis, $f = 50.8 \text{ mm}$) directed the light toward a $100 \mu\text{m}$ thick AgGaS_2 crystal (Eksma) for up-conversion with the gate pulse. More thorough discussions of the sample optics and the up-conversion setup are presented below.

Details of the Sample Optics. Since the samples are loose powders held in open containers (see below), they have to be placed facing up. To direct the beam downward toward the surface of the sample, the first parabolic mirror (OAP1) is rotated by $\sim 62^\circ$ about its optical axis (see Fig. 2). The sample is positioned so that its surface lies $\sim 12.7 \text{ mm}$ beyond the focus of OAP1 where the beam diameter has re-expanded to $\sim 5 \text{ mm}$. This is done to mitigate timing errors that could manifest due to surface irregularities (e.g., a variation in surface height of $20 \mu\text{m}$ can lead to a timing error approaching 100 fs). By placing the sample beyond the focus of OAP1, the height of the second parabolic mirror (OAP2) must be $\sim 6.35 \text{ mm}$ (roughly half the distance from the focus of OAP1 to the sample) lower than OAP1 in order to properly collect and re-collimate the scattered light.

Up-conversion Details. The diffusely reflected light was directed toward the AgGaS_2 (AGS) nonlinear crystal using OAP3 (Fig. 2). The crystal was cut for type I, non-collinear phase matching ($\theta = 82^\circ$, $\varphi = 45^\circ$).¹⁰ To avoid optical damage and continuum generation, the crystal was placed several millimeters before the focus of OAP3 where the beam diameter was $\sim 1 \text{ mm}$. The gate pulse was focused using a long focal length lens (L1, $f = 200 \text{ mm}$) and overlapped with the diffusely reflected light at an external angle of $\sim 38^\circ$. The diameter of the gate pulse at the point of overlap in the crystal was controlled by translating L1 along the optical axis.

The sum frequency is collected and focused into a $1/4 \text{ m}$ monochromator (Newport) with a 150 lines/mm grating

blazed at $4 \mu\text{m}$. The monochromator slits were set at $\sim 1 \text{ mm}$, corresponding to a large bandpass of $\sim 50 \text{ nm}$. In this capacity, the purpose of the monochromator was to filter out stray and ambient room light rather than to spectrally resolve the signal. The signal is detected using a photon-counting PMT (Hamamatsu, H8259-02) and digitized using a photon counter (Stanford Research Systems, SR400). The entire experimental setup is coordinated and controlled using a LabVIEW program written in-house.

Samples. Experiments were performed on four samples: pure KBr and KBr with varying concentrations (weight percentage) of carbon black (0.0097%, 0.033%, and 0.048%). Prior to use, the KBr was briefly dried in an oven for $\sim 1 \text{ h}$ at $\sim 120^\circ \text{C}$ followed by grinding in a ceramic mortar until the average particle diameter was $\sim 25 \mu\text{m}$ (measured under a low-power microscope with a calibrated reticle). Carbon black was used as received. For the combined samples, the appropriate amount of carbon black was added to the KBr and mixed thoroughly so that it evenly coated the KBr crystals.

To perform an experiment, a sample is placed in a shallow ($\sim 5 \text{ mm}$ depth) saucer-like ($\sim 25 \text{ mm}$ diameter) cup. In order to prepare a flat, uniform surface with minimal packing, the cups were slightly under-filled and covered with a small piece of glass (an old 2 in glass optical filter works well). The glass and cup were turned on end and lightly tapped one time. After returning them to the upright position, the glass was removed and the sample was carefully placed in the spectrometer.

Because of the inhomogeneous nature of the powdered samples, there can be considerable variation in signal intensities. Even a single sample, if removed from the spectrometer and then put back, will show very different intensities. Consequently, a quantitative comparison between samples is not possible. However, repeated experiments show that the temporal profiles are reproducible. This suggests that the optical proper-

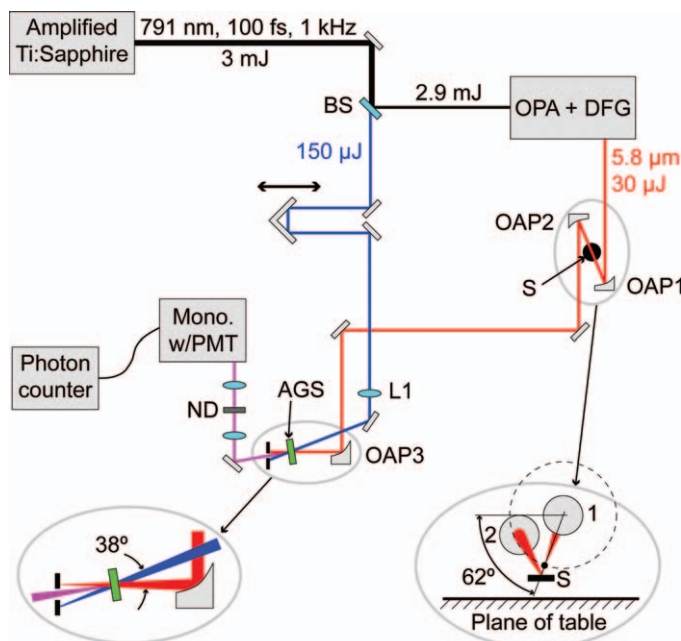


FIG. 2. Schematic of the instrument. See text for details.

ties of scattering samples could be estimated using a time-resolved approach rather than an intensity-based approach.

Data Collection and Analysis. A scan consisted of stepping the delay stage in 10 μm increments for a total distance of 7.2 mm. This corresponds to an optical increment of 6.67 fs and a total optical delay of 48 ps. At each stage position, the number of photons was integrated for 5 ns and then averaged over 100 laser shots. Counting was triggered using a signal from the 1 kHz oscillator. The delay between the trigger and the start of data collection was adjusted to maximize the count rate at the $t = 0$ position. Each scan was repeated three times and averaged.

An instrument response function was collected by using a mirror in place of the sample. In this context, the mirror is a “sample” that undergoes no diffuse reflection, and the resulting signal is just the cross correlation between the IR and gate pulses. Each scan was fit by convolving the instrument response with a bi-exponential function, $y = a_1e^{-t/\tau_1} + a_2e^{-t/\tau_2}$. The best fit was obtained using an iterative re-convolution algorithm.¹¹ It is important to emphasize that the data are normalized prior to fitting and that a_1 and a_2 in the bi-exponential equation are relative amplitudes.

The motivation for using a bi-exponential model to fit the data warrants a brief discussion. In the visible and near-IR spectral regions (and on slower time scales), diffuse reflection is typically modeled using the diffusion equation.^{12–14} All attempts to fit the data in this paper to the diffusion equation failed. This suggests that mid-IR diffuse reflection may not actually be diffusive in nature. In contrast to the diffusion equation, the agreement between the bi-exponential model and the data was excellent. While the bi-exponential model may not provide the same level of physical insight as the diffusion equation, it does provide a quantitative means to describe the data and identify characteristic features.

There is an inherent ambiguity in defining the speed of light for these experiments since the photons travel through air ($n = 1$) as well as the KBr matrix ($n = 1.5$). For this reason, we have opted to use the average of the two speeds, $c_{\text{avg}} = 0.25$ mm/ps, in all calculations requiring conversion between time and distance.

RESULTS AND DISCUSSION

Figure 3 shows the time-resolved data (circles) along with the best-fit curves (solid red lines). Two conclusions are immediately evident from the raw data: (1) the temporal profiles are clearly bi-exponential and (2) the fast component is dominant. The results of the bi-exponential fits are summarized in Fig. 4. Both time constants decrease linearly with increasing concentration of carbon black. The fast time constant (τ_1) ranges from ~ 0.7 ps for pure KBr to ~ 0.2 ps for KBr with 0.048% carbon black. Similarly, the slow time constant (τ_2) ranges from ~ 9 ps for pure KBr to ~ 5.5 ps for KBr with 0.048% carbon black.

However, the amplitudes behave very differently. While both vary linearly with increasing concentration of carbon black, the amplitude for the fast phase (a_1)

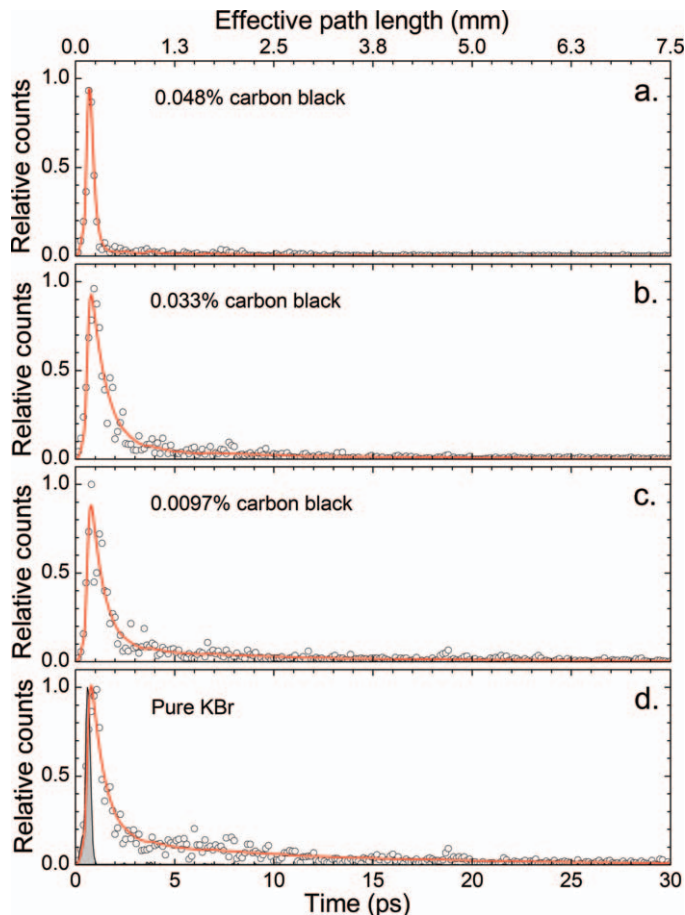


Fig. 3. Time-resolved data (circles) with bi-exponential fits (red curves). The gray shaded curve in the lower graph is the instrument response function. Plots (a), (b), (c), and (d) correspond to varying concentrations (weight percent) of carbon black; 0.048%, 0.033%, 0.0097%, and pure KBr, respectively.

increases while the amplitude for the slow phase (a_2) decreases. Moreover, a_1 accounts for $\sim 90\%$ of the total decay for pure KBr and increases to nearly 100% for KBr with 0.048% carbon black. In contrast, a_2 accounts for only $\sim 10\%$ of the decay for pure KBr but almost disappears entirely for KBr with 0.048% carbon black.

Also shown on Fig. 4 (using the right ordinate axes) are the corresponding effective path lengths for each phase. The slow phase corresponds to longer path lengths ranging from ~ 1.3 to 2.3 mm while the effective path lengths of the fast phase are about an order of magnitude shorter (~ 0.2 – 0.05 mm). However, because of the dominance of the fast phase, the overall mean effective path length (calculated using the mean time constant $a_1\tau_1 + a_2\tau_2$) is skewed toward the shorter range. What these results seem to suggest is that there are two characteristic “classes” of diffusely reflected mid-IR photons. The majority traverse relatively short distances corresponding to shallow penetration and/or less randomized motion. On the other hand, a smaller fraction ($< 10\%$) become trapped and travel longer distances, which could mean deeper penetration and/or a more random path. These two classes of photons are analogous to the so-called “ballistic” and “diffusive” photons that are typically observed in visible and near-IR

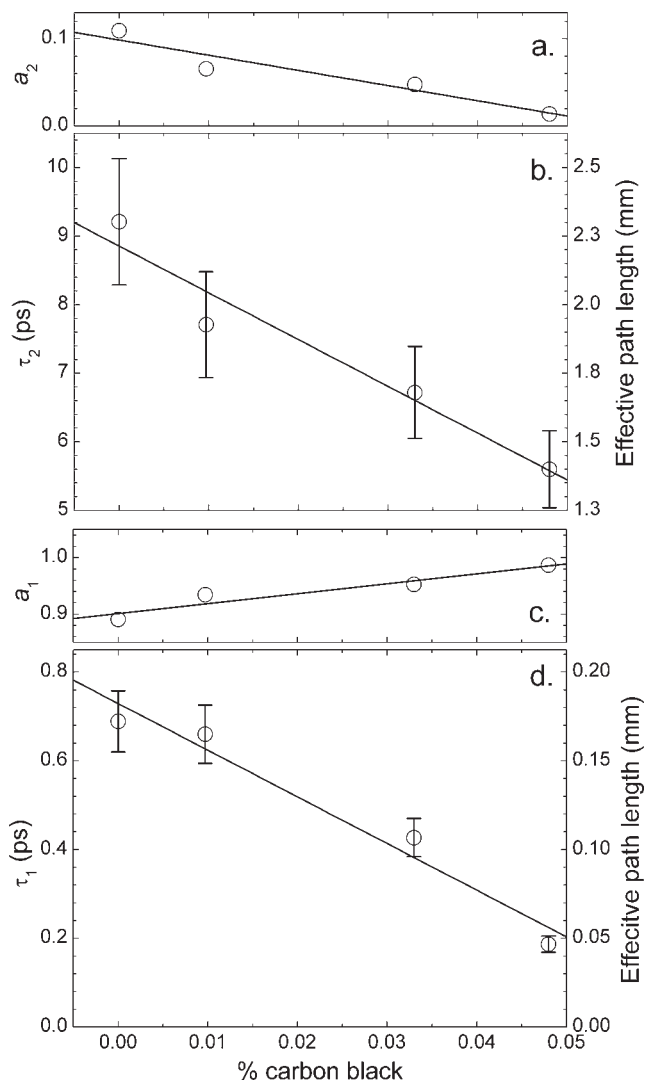


FIG. 4. Parameters from the bi-exponential fits. The slow time constant τ_2 and its amplitude a_2 are shown in plots (b) and (a), respectively. The fast time constant τ_1 and its amplitude a_1 are shown in plots (d) and (c), respectively.

diffuse reflection.^{15,16} However, given the potentially non-diffusive behavior of mid-IR photons on ultrafast time scales, this language is specifically avoided in this work.

CONCLUSION

This paper describes an instrument capable of studying mid-IR diffuse reflection on ultrafast time scales. Fast time resolution is achieved by up-converting the diffusely reflected mid-IR photons with an ultrafast gate pulse. The up-converted signal lies in the visible region of the spectrum so that a sensitive photomultiplier can be used for detection.

Experiments on powdered KBr samples containing varying amounts of carbon black were performed. In addition to demonstrating the instrument's capability, the

results of these experiments provide new insight into the underlying mechanism of mid-IR diffuse reflection. In particular, the results suggest that diffusely reflected mid-IR photons fall into two distinct categories. The majority (>90%) of the diffusely reflected photons follow relatively short paths (~ 0.1 mm), while the fraction that remains gets trapped in the matrix and traverses longer distances (~ 2 mm). This bimodal character could only have been identified using a time-resolved approach.

ACKNOWLEDGMENTS

This work was supported by the National Science Foundation under Grant No. CHE-0923583. The author would also like to thank Professor Peter R. Griffiths for his indispensable insight.

1. D.J. Dahm, K.D. Dahm. *Interpreting Diffuse Reflectance and Transmittance: A Theoretical Introduction to Absorption Spectroscopy of Scattering Materials*. Chichester, UK: IM Publications, 2007.
2. P.R. Griffiths, J.A. de Haseth. *Fourier Transform Infrared Spectrometry*. Hoboken, NJ: John Wiley and Sons, Inc., 2007. 2nd ed.
3. L.A. Averett, P.R. Griffiths. "Mid-Infrared Diffuse Reflection of a Strongly Absorbing Analyte on Non-Absorbing and Absorbing Matrices. Part I: Homogeneous Powders". *Appl. Spectrosc.* 2008. 62(4): 377-382.
4. C. Abrahamsson, J. Johansson, S. Andersson-Engels, S. Svanberg, S. Folestad. "Time-Resolved NIR Spectroscopy for Quantitative Analysis of Intact Pharmaceutical Tablets". *Anal. Chem.* 2005. 77(4): 1055-1059.
5. C. Abrahamsson, A. Lowgren, B. Stromdahl, T. Svensson, S. Andersson-Engels, J. Johansson, S. Folestad. "Scatter Correction of Transmission Near-Infrared Spectra by Photon Migration Data: Quantitative Analysis of Solids". *Appl. Spectrosc.* 2005. 59(11): 1381-1387.
6. F. Chauchard, J.M. Roger, V. Bellon-Maurel, C. Abrahamsson, S. Andersson-Engels, S. Svanberg. "MADSTRESS: A Linear Approach for Evaluating Scattering and Absorption Coefficients of Samples Measured Using Time-Resolved Spectroscopy in Reflection". *Appl. Spectrosc.* 2005. 59(10): 1229-1235.
7. D.T. Delpy, M. Cope, P. van der Zee, S. Arridge, S. Wray, J. Wyatt. "Estimation of Optical Pathlength Through Tissue from Direct Time of Flight Measurement". *Phys. Med. Biol.* 1988. 33(12): 1433-1442.
8. J. Johansson, S. Folestad, M. Josefson, A. Sparen, C. Abrahamsson, S. Andersson-Engels, S. Svanberg. "Time-Resolved NIR/Vis Spectroscopy for Analysis of Solids: Pharmaceutical Tablets". *Appl. Spectrosc.* 2002. 56(6): 725-731.
9. S. Tsuchikawa, S. Tsutsumi. "Application of Time-of-Flight Near-Infrared Spectroscopy to Wood with Anisotropic Cellular Structure". *Appl. Spectrosc.* 2002. 56(7): 869-876.
10. V.G. Dmitriev, G.G. Gurzadyan, D.N. Nikogosyan. *Handbook of Nonlinear Optical Crystals*. Berlin Heidelberg: Springer-Verlag, 1997. 2nd ed.
11. D.J.S. Birch, R.E. Imhof. "Time-Domain Fluorescence Spectroscopy Using Time-Correlated Single-Photon Counting". In: J.R. Lakowicz, editor. *Topics in Fluorescence Spectroscopy*. New York, NY: Plenum Press, 1991. Vol. 1. Pp. 1-95.
12. W. Cai, M. Xu, M. Lax, R.R. Alfano. "Diffusion Coefficient Depends on Time, not on Absorption". *Opt. Lett.* 2002. 27(9): 731-733.
13. M.S. Patterson, B. Chance, B.C. Wilson. "Time Resolved Reflectance and Transmittance for the Noninvasive Measurement of Tissue Optical Properties". *Appl. Opt.* 1989. 28(12): 2331-2336.
14. R. Pierrat, J.J. Greffet, R. Carminati. "Photon Diffusion Coefficient in Scattering and Absorbing Media". *J. Opt. Soc. Am. A.* 2006. 23(5): 1106-1110.
15. B.B. Das, F. Liu, R.R. Alfano. "Time-Resolved Fluorescence and Photon Migration Studies in Biomedical and Model Random Media". *Rep. Prog. Phys.* 1997. 60(2): 227-292.
16. M. Sormaz, P. Jenny. "Contrast Improvement by Selecting Ballistic-Photons Using Polarization Gating". *Opt. Express.* 2010. 18(23): 23746-23755.